SELF-SUPERVISED IMAGE DENOISING WITH SWIN TRANSFORMER

Pavel Chizhov, Mikhail Papkov
Institute of Computer Science, University of Tartu
Tartu, Estonia
{pavel.chizhov,mikhail.papkov}@ut.ee

ABSTRACT

Self-supervised image denoising aims to reconstruct signal from a noisy image with no additional information. Typically, this is accomplished by means of specific frameworks built upon fully-convolutional neural networks. In two such frameworks, Noise2Self and Noise2Same, we replaced conventional convolutional backbones with a state-of-the-art Swin Transformer-based model. In this paper, we summarize the results of experiments on a range of datasets and examine the advantages and limitations of transformers in self-supervised denoising.

1 INTRODUCTION AND RELATED WORK

Deep learning solutions for *self-supervised* denoising are usually based on a fully-convolutional U-Net architecture (Ronneberger et al., 2015). It was used in Noise2Void (Krull et al., 2019) and Noise2Self (Batson & Royer, 2019), which concurrently introduced masked pixels reconstruction as a proxy task for blind-spot denoising. The main limitation of masking was the inability to look at pixels' own noisy albeit useful signal. Noise2Same (Xie et al., 2020) addressed this issue with a dual forward pass of masked and unmasked images through the network.

SwinIR (Liang et al., 2021) is a state-of-the-art model for *supervised* image restoration, including denoising, based on Swin Transformer (Liu et al., 2021). Despite the superiority of this architecture, there was limited research exploring its capabilities in the self-supervised setting. DnT (Liu et al., 2022) utilized a variant of SwinIR for *unsupervised single-image* denoising, following R2R (Pang et al., 2021) to sample pairs of images with independent noise. In this work, we propose a simpler approach to validate SwinIR performance for self-supervised denoising by directly integrating it into Noise2Self and Noise2Same frameworks. Additionally, we conduct an ablation study to determine optimal hyperparameters on a range of datasets.

2 METHODS

Noise2Self uses a blind-spot loss — a mean squared error (MSE) between predicted and hidden values of masked pixels. Noise2Same makes an additional run through the model when the unchanged image is passed as input. In this case, the loss consists of two components: reconstruction MSE between the second output and the noisy input and invariance MSE between the two outputs computed over the pixel mask. The difference between frameworks is illustrated in Figure 2.

SwinIR model (Figure 3) consists of six groups with six Swin Transformer blocks in each group, followed by a 3×3 convolution. Two consequent blocks alternate between plain and shifted window multi-head self-attention. We used window size 16×16 and patch size 1×1 pixels, and did not use the global shortcut (adding input to output). We further discuss training details in Appendix B.

3 EXPERIMENTS AND DISCUSSION

The models were trained and evaluated on three noise datasets: BSD68 — grayscale images of natural objects (Martin et al., 2001), HanZi — grayscale images of handwritten Chinese characters (Batson & Royer, 2019), and ImageNet — RGB images of natural objects (Deng et al., 2009; Xie et al., 2020). We followed Xie et al. (2020) for training settings and data preparation, except for BSD68, where we used crops of size 128×128 and batch size 32 instead of 64×64 and 64.

Table 1: Denoising results. The best scores are highlighted in bold, and the second-best scores are underlined. We report the results of our implementation wherever possible and compare them to those reported in Noise2Same (Xie et al., 2020). † — clipping gradient norm to 1.0.

Method	Backbone	BSD68		HanZi		ImageNet	
		PSNR	SSIM	PSNR	SSIM	PSNR	SSIM
Noise2Void	U-Net (Xie et al., 2020)	27.71	—	13.72	—	21.36	—
Noise2Self	U-Net (Xie et al., 2020)	26.98	—	13.94	—	20.38	—
	U-Net	26.88	0.734	14.16	<u>0.512</u>	21.33	0.574
	SwinIR	27.57	0.774	13.57	0.475	20.28†	0.524†
Noise2Same	U-Net (Xie et al., 2020)	27.95	—	<u>14.38</u>	—	22.26	—
	U-Net	**28.11**	<u>0.781</u>	**14.85**	**0.542**	<u>22.85</u>	<u>0.625</u>
	SwinIR	<u>28.07</u>	**0.786**	14.35	0.513	**23.05**	**0.635**

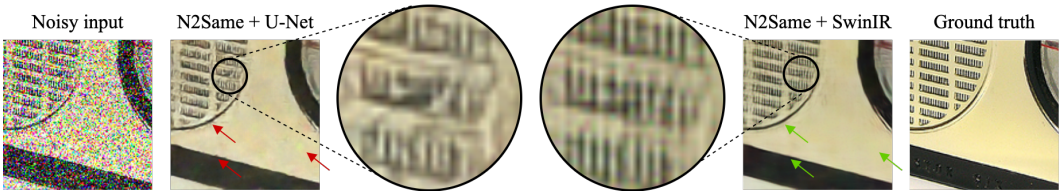

Figure 1: Image restoration results of U-Net and SwinIR in Noise2Same self-supervised framework.

The evaluation results are given in Table 1. SwinIR backbone improved the peak signal-to-noise ratio (PSNR) and structural similarity index (SSIM) in several experiments, such as Noise2Same on ImageNet ($+0.20$ PSNR) or Noise2Self on BSD68 ($+0.69$ PSNR). In Noise2Same on BSD68, SwinIR has a slightly lower PSNR but better SSIM. We hypothesize that SwinIR is more capable of detailed structure restoration than U-Net. In Figure 1, high-frequency details are better retained in the output of SwinIR. At the same time, in the picture produced by U-Net, the structure is blurry and uneven. As an exclusive case, however, HanZi dataset has a clear black background and less high-frequency signal than natural images — SwinIR did not improve its scores.

Being more computationally expensive than U-Net, SwinIR has its limitations regarding resources and processing time. We document the details in Appendix C, Tables 3 and 4.

Ablations. By default, SwinIR (Liang et al., 2021) embeds patches of size 1×1 px instead of 4×4 originally proposed in Swin Transformer (Liu et al., 2021). While this is an essential change for the image restoration task, it implicitly reduces window resolution from 28×28 to 7×7. Such window size is not computationally efficient, because input should be padded for divisibility (e.g., crop 64×64 will increase in size by 19.6%). Also, it may be too small for the image restoration task. We compared window sizes 8×8 and 16×16 and found that the larger one consistently improves the scores (see Table 6). We have also investigated the importance of larger crop sizes against larger batch sizes and found that crops of size 128×128 with batch size 32 are better than 64×64 and 64 on BSD68 for all backbones and frameworks except U-Net in Noise2Self (see Table 5).

4 Conclusion

We replaced a fully-convolutional architecture with a transformer-based model in self-supervised image denoising frameworks and assessed the results. Our experiments showed that SwinIR demonstrates competitive performance, being capable of restoring complex high-frequency details ignored by its convolutional counterparts. However, such improvement comes at a considerable computational cost. We did not experiment with 3D data, and it is yet unclear if it is feasible to denoise it with transformers. we leave this question open for further work.

URM STATEMENT

The authors acknowledge that at least one key author of this work meets the URM criteria of the ICLR 2023 Tiny Papers Track.

REFERENCES

Joshua Batson and Loic Royer. Noise2Self: Blind denoising by self-supervision. In Kamalika Chaudhuri and Ruslan Salakhutdinov (eds.), *Proceedings of the 36th International Conference on Machine Learning*, volume 97 of *Proceedings of Machine Learning Research*, pp. 524–533. PMLR, 09–15 Jun 2019. URL https://proceedings.mlr.press/v97/batson19a.html.

Jia Deng, Wei Dong, Richard Socher, Li-Jia Li, Kai Li, and Li Fei-Fei. Imagenet: A large-scale hierarchical image database. In *2009 IEEE Conference on Computer Vision and Pattern Recognition*, pp. 248–255, 2009. doi: 10.1109/CVPR.2009.5206848.

Diederik P Kingma and Jimmy Ba. Adam: A method for stochastic optimization. *arXiv preprint arXiv:1412.6980*, 2014.

Alexander Krull, Tim-Oliver Buchholz, and Florian Jug. Noise2void-learning denoising from single noisy images. In *Proceedings of the IEEE/CVF Conference on Computer Vision and Pattern Recognition*, pp. 2129–2137, 2019.

Jingyun Liang, Jiezhang Cao, Guolei Sun, Kai Zhang, Luc Van Gool, and Radu Timofte. Swinir: Image restoration using swin transformer. *arXiv preprint arXiv:2108.10257*, 2021.

Xiaolong Liu, Yusheng Hong, Qifang Yin, and Shuo Zhang. Dnt: Learning unsupervised denoising transformer from single noisy image. In *Proceedings of the 4th International Conference on Image Processing and Machine Vision*, IPMV '22, pp. 50–56, New York, NY, USA, 2022. Association for Computing Machinery. ISBN 9781450395823. doi: 10.1145/3529446.3529455. URL https://doi.org/10.1145/3529446.3529455.

Ze Liu, Yutong Lin, Yue Cao, Han Hu, Yixuan Wei, Zheng Zhang, Stephen Lin, and Baining Guo. Swin transformer: Hierarchical vision transformer using shifted windows. In *Proceedings of the IEEE/CVF International Conference on Computer Vision (ICCV)*, 2021.

D. Martin, C. Fowlkes, D. Tal, and J. Malik. A database of human segmented natural images and its application to evaluating segmentation algorithms and measuring ecological statistics. In *Computer Vision, 2001. ICCV 2001. Proceedings. Eighth IEEE International Conference on*, volume 2, pp. 416–423 vol.2, 2001. doi: 10.1109/ICCV.2001.937655. URL http://ieeexplore.ieee.org/xpls/abs_all.jsp?arnumber=937655.

Tongyao Pang, Huan Zheng, Yuhui Quan, and Hui Ji. Recorrupted-to-recorrupted: unsupervised deep learning for image denoising. In *Proceedings of the IEEE/CVF conference on computer vision and pattern recognition*, pp. 2043–2052, 2021.

Adam Paszke, Sam Gross, Soumith Chintala, Gregory Chanan, Edward Yang, Zachary DeVito, Zeming Lin, Alban Desmaison, Luca Antiga, and Adam Lerer. Automatic differentiation in pytorch. 2017.

Alex Rogozhnikov. Einops: Clear and reliable tensor manipulations with einstein-like notation. In *International Conference on Learning Representations*, 2022. URL https://openreview.net/forum?id=oapKSVM2bcj.

Olaf Ronneberger, Philipp Fischer, and Thomas Brox. U-net: Convolutional networks for biomedical image segmentation. In Nassir Navab, Joachim Hornegger, William M. Wells, and Alejandro F. Frangi (eds.), *Medical Image Computing and Computer-Assisted Intervention – MICCAI 2015*, pp. 234–241, Cham, 2015. Springer International Publishing. ISBN 978-3-319-24574-4.

Yaochen Xie, Zhengyang Wang, and Shuiwang Ji. Noise2Same: Optimizing a self-supervised bound for image denoising. In *Advances in Neural Information Processing Systems*, volume 33, pp. 20320–20330, 2020.

A ARCHITECTURES

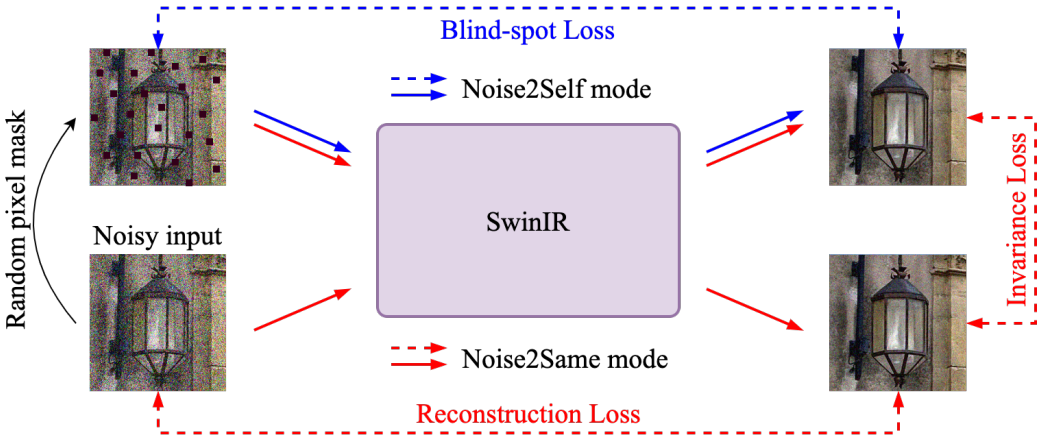

Figure 2: Noise2Self (Batson & Royer, 2019) and Noise2Same (Xie et al., 2020) frameworks.

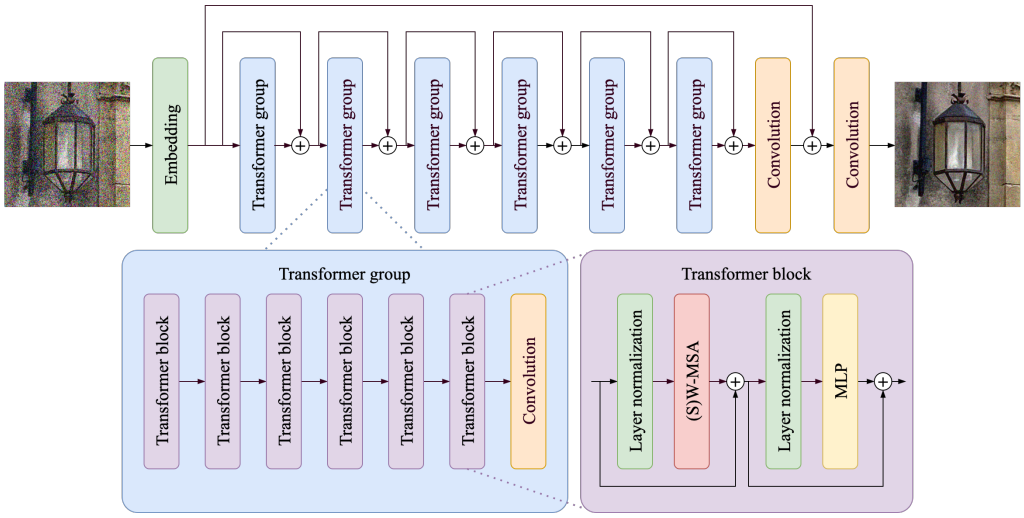

Figure 3: SwinIR (Liang et al., 2021) model architecture.

B TRAINING DETAILS

We used Adam optimizer (Kingma & Ba, 2014) in all experiments with initial learning rate of $4 \cdot 10^{-4}$ and scheduled learning rate decay by half every 5000 iterations. The main training setup parameters are demonstrated in Table 2. We encountered a problem of exploding gradients in Noise2Self + SwinIR on HanZi with window size of 8×8 and on Imagenet. In these cases, we had to use gradient norm clipping of 1.0.

We implemented all models in Python 3.8.3 and PyTorch 1.12.1 (Paszke et al., 2017), and trained them on NVIDIA A100 80GB GPUs (driver version: 470.57.02, CUDA version: 11.4). We used `einops` (Rogozhnikov, 2022) library to implement transformer blocks in a verbose way.

C COMPUTATIONAL COSTS

SwinIR is a more computationally expensive model than U-Net, so it was trained longer on multiple GPUs (see Tables 3 and 4 for details).

Table 2: Training configuration.

	BSD68	HanZi	ImageNet
Batch size	32	64	64
Training crop size	128	64	64
# iterations	80000	50000	50000

Table 3: Number of GPUs utilized in each experiment.

Method	Backbone	BSD68	HanZi	ImageNet
Noise2Self	U-Net	1	1	1
	SwinIR	4	2	2
Noise2Same	U-Net	1	1	1
	SwinIR	8	4	4

Table 4: Training time (TT) and average inference time (AIT) in experiments. Inference was done in a single thread with batch size 1, as for BSD68 and ImageNet it is infeasible to compose batches due to varying image sizes.

		BSD68		HanZi		ImageNet	
Method	Backbone	TT (h)	AIT (ms)	TT (h)	AIT (ms)	TT (h)	AIT (ms)
Noise2Self	U-Net	1	7	0.5	5	1	15
	SwinIR	20	2632	12	40	14	11565
Noise2Same	U-Net	2	8	1	6	1	14
	SwinIR	26	3548	22	57	13	5985

D ABLATION STUDY

Table 5: BSD68 training crop and batch size ablation study. The scores are compared within each method and backbone combination. The best scores are highlighted in bold.

Method	Backbone	Crop size	Batch size	PSNR	SSIM
Noise2Self	U-Net	64	64	**26.94**	**0.743**
		128	32	26.88	0.734
	SwinIR	64	64	27.49	0.769
		128	32	**27.57**	**0.774**
Noise2Same	U-Net	64	64	27.90	0.752
		128	32	**28.11**	**0.781**
	SwinIR	64	64	27.78	0.736
		128	32	**28.07**	**0.786**

Table 6: Window size ablation study. The scores are compared across window sizes of SwinIR in each method separately. The best scores are highlighted in bold. † — clipping gradient norm to 1.0.

Method	Window size	BSD68 PSNR	BSD68 SSIM	HanZi PSNR	HanZi SSIM	ImageNet PSNR	ImageNet SSIM
Noise2Self	8	27.54	0.772	12.18†	0.388†	19.41†	0.470†
	16	**27.57**	**0.774**	**13.57**	**0.475**	**20.21**†	**0.493**†
Noise2Same	8	28.00	**0.786**	14.24	0.510	22.95	0.626
	16	**28.07**	**0.786**	**14.35**	**0.513**	**23.05**	**0.635**

E ADDITIONAL EXAMPLES

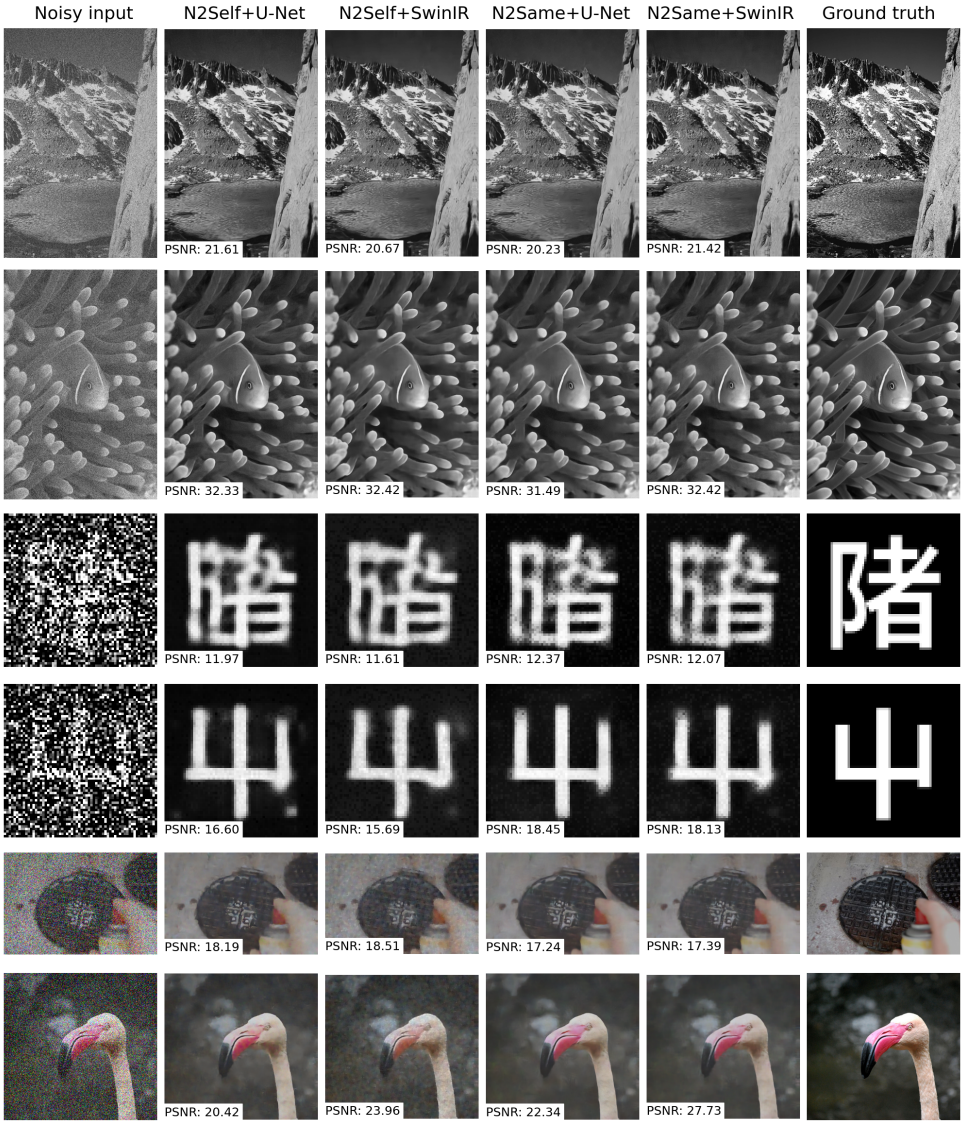

Figure 4: Additional examples of images denoised in BSD68 (first pair of rows), HanZi (second pair of rows), and ImageNet (last pair of rows) experiments. Each pair of rows contains a hard and a simple example from the dataset with the corresponding PSNR scores.